



**HAL**  
open science

# Lifetime of timber notched beams under several random modelling of french climates

Myriam Chaplain, Denys Breysse, Antoine Marache

► **To cite this version:**

Myriam Chaplain, Denys Breysse, Antoine Marache. Lifetime of timber notched beams under several random modelling of french climates. WCTE 2012, Jul 2012, Auckland, New Zealand. hal-03515579

**HAL Id: hal-03515579**

**<https://hal.science/hal-03515579>**

Submitted on 6 Jan 2022

**HAL** is a multi-disciplinary open access archive for the deposit and dissemination of scientific research documents, whether they are published or not. The documents may come from teaching and research institutions in France or abroad, or from public or private research centers.

L'archive ouverte pluridisciplinaire **HAL**, est destinée au dépôt et à la diffusion de documents scientifiques de niveau recherche, publiés ou non, émanant des établissements d'enseignement et de recherche français ou étrangers, des laboratoires publics ou privés.

## LIFETIME OF TIMBER NOTCHED BEAMS UNDER SEVERAL RANDOM MODELLING OF FRENCH CLIMATES

Myriam Chaplain<sup>1</sup>, Denys Breyse<sup>2</sup>, Antoine Marache<sup>3</sup>

**ABSTRACT:** The mechanical response and durability of building materials is highly influenced by the atmospheric conditions. Temperature and air humidity have a great influence on the transfer of water and contaminants in the porous structure of these materials. This paper focuses on the effects of moisture content and/or moisture dynamics which are even more important when rupture is due to crack. Climatic variations are simulated and a lifetime model is proposed. The “climat” method consists in processing a wide amount of meteorological records from four French sites covering different climates, in order to identify their statistical properties, identify their time auto-correlation characteristics, be able to rebuild synthetic signals with the same or different characteristics. The generic model is able to reproduce a very large amount of simulations, which is necessary for reliability or statistical analyses. The lifetime model predicts the incubation time and the time of crack propagation until the failure. As temperature has a smaller influence on the time to failure than relative humidity, its effects are not directly taken into account in the model. Predictions of the proposed model for various air humidity simulations are compared with creep test results obtained on notched LVL beams under various climatic conditions.

**KEYWORDS:** wood, weather modelling, crack initiation and propagation, duration of load modelling

### 1 INTRODUCTION

Environmental parameters like air temperature and relative humidity have a high influence on the response of timber constructions and their durability. Thus it seems useful to try to better estimate the possible influence of global change scenarios on the durability of materials and induced costs, because of a more expensive maintenance. Many models exist yet which describe how environmental parameters can influence durability. The focus is given here on the modelling of input data for such models, namely temperature and air humidity. The climatic variability at various space and time-scales is an issue of interest for many reasons in civil engineering and building. It must be accounted for when one tries to optimize the design. Air temperature and humidity variations have also a main influence on the ageing processes of building materials, either because they directly influence material properties or because they govern heat and mass transfers. It is the

case for timber durability since the ambient variations govern mould growth [13], creep and crack propagation [3, 4, 6...].

### 2 CLIMATE MODELLING

Twelve-year database at the time step of one hour of temperature and relative humidity have been recorded in four regions of France: Atlantic (Bordeaux), Brittany (Brest), Auvergne (Clermont-Ferrand), Mediterranean (Corsica - Ajaccio). For each climate, a model of the time variations has been developed. Such a model enables to simulate the material response in a given environment and to study what can be this response in different scenarios, like those corresponding to global warming. Even if the meteorological processes have not been modelled explicitly at the regional scale, the weather model is able to reproduce [3, 17, 19]:

- the seasonal variations for the two variables,
- the day/night fluctuations, with cycles in the Temperature (T) - Relative humidity (RH) diagram, reproducing the humid air physics,
- the time memory of the random part of the local weather, which exhibits some temporal autocorrelation at a time scale below five days, for both T and RH.

---

<sup>1</sup> Myriam Chaplain, Univ. Bordeaux 1, I2M/GCE, UMR 5295, A11 ; 351 cours de la Libération, F-33405 Talence, France. Email: m.chaplain@I2m.u-bordeaux1.fr

<sup>2</sup> Denys Breyse, Univ. Bordeaux 1, I2M/GCE, UMR 5295, B18, Avenue des Facultés, F-33405 Talence, France. Email: d.breyse@I2m.u-bordeaux1.fr

<sup>3</sup> Antoine Marache, Univ. Bordeaux 1, I2M/GCE, UMR 5295, B18, Avenue des Facultés, F-33405 Talence, France. Email: a.marache@I2m.u-bordeaux1.fr

## 2.1 MODELLING TEMPERATURE AND HUMIDITY

The Relative Humidity RH is considered as a random variable whose variations are constrained by temperature values and physical laws (air saturation). To obtain RH, an important part of the modeling is the simulation of the temperature.

### 2.1.1 Temperature modelling

We considered that time variation for temperature writes  $T(t)$  can be written as (1):

$$T(t) = T_{D1}(t) + T_{D2}(t) + T_A(t) \quad (1)$$

where  $T_{D1}(t)$  and  $T_{D2}(t)$  are two deterministic components linked with seasonal and daily natural variations (driven by astronomic constraints) and where  $T_A(t)$  is a stochastic signal, whose characteristic have to be identified. This part will explain the statistical variability between consecutive days, but also between years at a given date. It corresponds to the non-deterministic part of the climate and it is due to atmospheric phenomena at small time-scales (due to air masses movements at the scale of few days) and from local processes (role of vegetation...). The magnitude and the time correlation of this stochastic signal have both be identified from the data base of weather records from 1997 to 2011 on four INRA sites.

#### Modelling the deterministic $T_{D1}$ and $T_{D2}$ temperature

The deterministic part is easier to identify on an averaged year signal, since averaging reduces the variability:

$$T_m(t) = [ \sum T_i(t) ] / n \quad (2)$$

where  $n$  is the number of recorded years, here 13. The seasonal component  $T_{D1}(t)$  of Equation (1) is modelled with a sine function:

$$T_{D1}(t) = T_{ref} + M_T \cdot \sin [ 2\pi(t - t_o)/8760 ] \quad (3)$$

Table 1 synthesizes what parameters have been identified for the 3 climates.

**Table 1:** Determinist temperature  $T_{D1}$  parameters

	Aquitaine	Brittany	Corsica	Auvergne
Model parameters				
$T_{ref}$	12.8	11.9	16.0	7.8
$M_T$	7.0	5.3	7.2	7.7
$t_o$	2600	2280	2810	2710
(min. day)	(jan, 18)	(jan, 4)	(jan, 26)	(jan, 22)

From Equations (1), (2) and (3),  $T_{D2}(t)$  can be identified by studying the deterministic part of the residual  $T_{res1}(t)$  :

$$T_{res1}(t) = T_m(t) - T_{D1}(t). \quad (4)$$

$T_{D2}(t)$  is a zero-mean signal which describes the day/night variations. It is governed by the solar radiations intensity and by the air refreshing during the night. This variation is modeled considering that there is

a linear decrease of the temperature between sunset ( $t_{ss}$ ) and next sunrise ( $t_{sr}$ ) and that a linear + half-sine function describes the temperature variation during the day time [3]. More sophisticated models have been proposed in the literature, but all models suffer from the same weakness, that of being unable to reproduce daily variations in case of overcast days [19]. It is the reason why, in most usual weather generators, a first step consists in separating at the very beginning of the process dry days from days with precipitation [20].

The values of  $t_{ss}$  and  $t_{sr}$  are explicit functions of the day and of the longitude and latitude, the difference of this  $t_{xo}$  time ( $t_{ss}-t_{sr}$ ) giving the daylight duration  $D$ . The  $T_{D2}(t)$  model considers that the daily minimum temperature occurs at sunrise. It has only two parameters: the temperature  $\Delta T$ , difference between sunrise and sunset temperature, and the amplitude of the half-sine function  $A$ . Writing that the signal is zero mean determines how the signal is positioned around the mean value, for instance by expressing the temperature at sunrise:

$$T(t_{sr}) = - \Delta T/2 - D (A - \Delta T/2) / 12 \pi \quad (5)$$

The values of  $A$  and  $\Delta T$  varies along the year, since the daily magnitude of temperature variations depends on the day length. Figure 1 compares the  $T_{D2}(t)$  signal to a real record along three consecutive days and confirms the ability of the  $T_{D2}(t)$  model to describe the daily temperature variations.

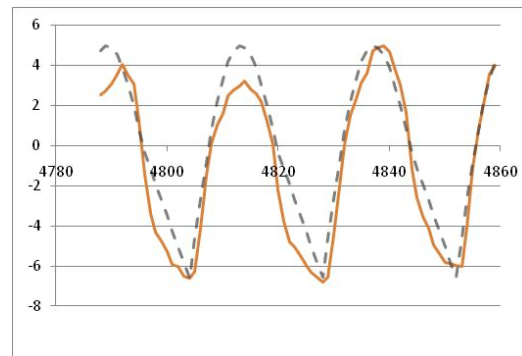


**Figure 1:** Daily temperature variations at the scale of 3 days:  $T_{D2}(t)$  model (dotted curve) and  $T_m(t) - T_{D1}(t)$  signal (hour count on x-axis)

#### Modelling the stochastic temperature variations

As an example, figure 2 shows the stochastic residual for the year 2003 in Bordeaux. This year is the warmer of the time series (the average temperature had been 0.6°C higher than the average value for the whole data set). It can be seen that the temperature at a given time can be 10°C higher or 10°C lower than the expected value, this difference being more than 15°C in extreme periods. For instance, France has known in July 2003 an extreme period of hot temperatures, which is clearly visible on the figure 2, when the measured temperature was 5°C to 15°C higher than usual during a full decade.

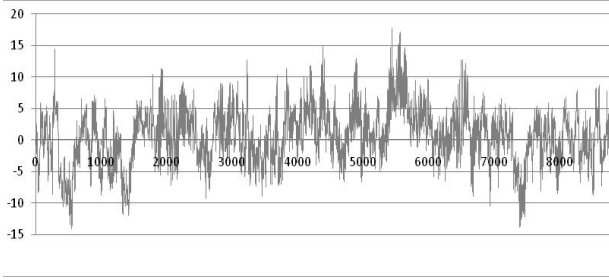


**Figure 2:** Stochastic part of the temperature, year 2003 (hour count on x-axis) in Bordeaux

The next step is the characterization of this stochastic residual. The method used here is that of variographical analysis, which comes to compute the experimental semi-variogram function for each year:

$$\gamma(h) = (\sum [T_A(t+h) - T_A(t)]^2) / (2 N(h)) \quad (6)$$

where  $h$  is the delay between two measurements (or lag-) and  $N(h)$  the number of pairs of data for a given  $h$  value. The average yearly variances of these stochastic signals is amounts respectively 17.2, 10.2, 7.1 and 20.5°C<sup>2</sup> for Bordeaux, Brittany, Corsica and Clermont-Ferrand. Figure 3 plots the semi-variograms identified for 14 years of record in Bordeaux, the average variogram and the model variogram. In this case, the model is exponential.

The same type of results has been obtained for the four data series, with a progressive loss of correlation with time log. A kind of periodic variation (with a period equal 24 hours) superimposes to this behaviour. It results from the fact that the deterministic signal  $T_{D2}(t)$  has considered an “average day”, not accounting for the difference between sunny days and overcast days.

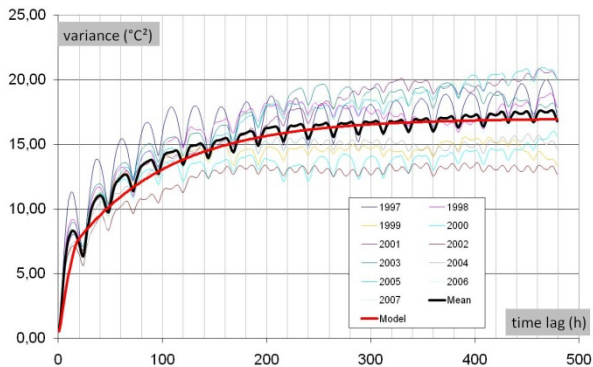


**Figure 3:** Experimental variograms and model variogram (Bordeaux case)

About half of the correlation is lost after 24 hours and 90 % of the correlation is lost after about 5 to 6 days. After such a delay, there is no more correlation between two temperature measurements. The correlation time is of prime importance for the temperature variability, since it represents the « memory » of the stochastic fluctuations, very probably due to the atmospheric phenomena at a regional scale, which have not been explicitly modeled. The synthetic signals must of course

reproduce this characteristic pattern. The identified time scale can be compared to that found by [11] with a different approach, since they identified a 5 days memory in an auto-regressive model for temperature. The temporal random fluctuations of wind velocity, which are also linked to circulations at a regional scale, are considered to lose their correlation after a delay from 4 to 12 days, with a mean value of 8 days in the northern hemisphere [14]. The correlation coefficient  $\rho$  used for temperature on two consecutive days in time series processes is usually about 0.60 to 0.80, which corresponds to  $\rho^2 = 0.4$  to 0.7, and to a loss of correlation of about 30 to 60 % [2, 15].

### 2.1.2 Absolute Humidity Modelling

The time variations of absolute humidity are governed by two physical processes:

- ✓ the condensation process, as discussed above,
- ✓ the movement of air masses because of the wind.

Reproducing this influence requires a physical model at another scale. It is not considered directly here.

The choice is to consider a reference time for each day:  $t_{ref} = 1$  p.m., roughly corresponding to the sun maximal elevation, to the daily maximal temperature and daily minimal potential absolute humidity. The corresponding reference value for absolute humidity  $x_{ref}$  is calculated as:

$$x_{ref} = [\sum x(i)]/5, i = 11 \text{ a.m. to } 3 \text{ p.m. (step 1 hour)} \quad (7)$$

$x_{ref}$  and  $T_{ref}$  (which is the temperature at the same time) appear to be statistically linked. Their correlation can be identified from data bases as well as the conditional distribution  $p(x_{ref}|T_{ref})$ . For synthetic signals, the choice is, once  $T_{ref}$  has been generated, to conditionally generate  $x_{ref}$ . Finally, the hourly variations between  $x_{ref}$  (day) and  $x_{ref}$  (day+1) are interpolated. At any time, it is checked that the pair  $\{T(h), x(h)\}$  is compatible with the saturation curve. These two variables are distributed in a large domain, and their distribution is constrained by the (upper) saturation curve (Fig. 4).

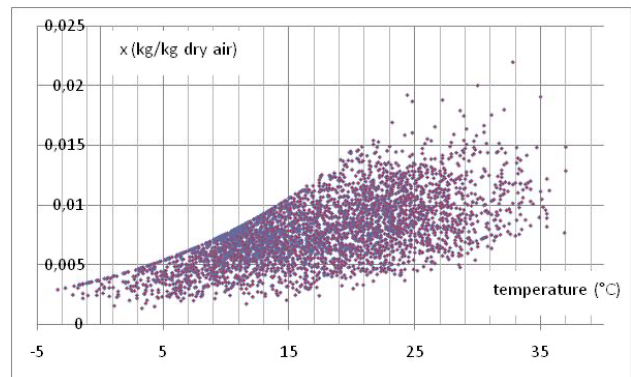


**Figure 4:** Correlation between  $x_{ref}$  and  $T_{ref}$  (from 3850 data from 11 years of records in Bordeaux)

The simulation process is the following:

- the conditional distribution  $p(x_{ref}|T_{ref})$  is identified from original records. For any small interval around  $T_{ref}$ , the

mean value  $m(x_{ref})$  and coefficient of variation  $cv(x_{ref})$  are calculated from the empirical data,

- empirical polynomial relationships are identified:  $m(x_{ref}) = f_1(T_{ref})$  and  $cv(x_{ref}) = f_2(T_{ref})$ , to fit experimental results,
- $x_{ref}$  is assumed to follow a Gaussian distribution  $\mathcal{N}(m(x_{ref}), cv(x_{ref}))$ , with additional restrictions so as to avoid too small values or values exceeding the saturation, which are not physically possible.

Thus, for each  $T_{ref}$  value which has been generated by the synthetic temperature generator,  $x_{ref}$  can be generated accordingly. Once  $x_{ref}$  has been generated, a linear interpolation between  $x_{ref}$  values on two consecutive days is performed, with respect to the T signal and the saturation curve.

More details of the proceeding is developed by Breyse et al in [3] for Bordeaux climate.

### 2.1.3 Relative Humidity Modelling

The Relative Humidity HR is obtained from the absolute humidity x:

$$x = 0.622 p_{vap} / (760 - p_{vap}) \text{ with } p_{vap} = HR p_{sat} \quad (8)$$

where  $p_{vap}$  is the water vapour pressure in mmHg,  $p_{sat}$  is the water vapour pressure at saturation

$p_{sat}$  pressure depends on the temperature, with a relation which can be expressed according to an empirical law, like the Dupré formula:

$$p_{sat} = \exp [46.784 - 6435/T_{abs} - 3.868 \ln(T_{abs})] \quad (9)$$

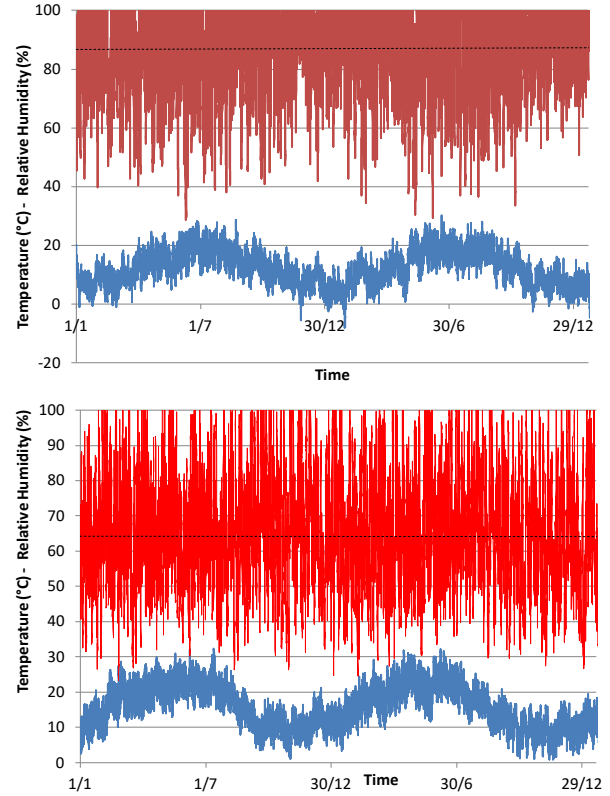
where  $T_{abs}$  is the absolute temperature in Kelvin and where  $p_{sat}$  is expressed in mmHg (the vapour pressure in hPa can be obtained by multiplying by a factor 1000/760).

Figure 5 presents two simulations of extreme French climates over a lag of three years: the first is a Brittany climate which is a humid atmosphere –average RH around 87%, the second is a Corsica climate which average humidity RH is near 65%. In Brittany, external LVL elements have average moisture almost always equal to the saturated moisture.

Average simulated RH are closed to recorded observation excepted for Corsica: the model based on the determination of RH from the modelling of the temperature gives lower humidity when the temperature is high like in Mediterranean region.

**Table 2:** average RH and moisture for 4 regions: recorded / simulations

	Average RH	
	recorded	simulation
Atlantic (Bordeaux)	77%	79%
Brittany	86%	87%
Corsica	72 %	66%
Auvergne	78%	80%



**Figure 5:** Example of predicted climates (relative humidity RH and temperature) on top Brittany weather, below Mediterranean weather

## 2.2 RELATIVE HUMIDITY – MOISTURE RELATIONSHIP

First, the moisture content in mass at the surface of a beam is assumed to be equal to the equilibrium moisture content ( $w_{eq}$ ) of the material obtained from the iso-sorption curves. In this study, we use the iso-sorption curve of a reconstituted LVL spruce wood (LVL, Laminated Veneer Lumber) we obtained at a temperature of 20°C. For the LVL, the adsorption and desorption curves are close, so, to simplify our modelling, we only consider that adsorption and desorption moisture isotherm follow the same curve. The effect of temperature on moisture isotherms is also neglected in this first approach [12]. The specimens are LVL notched beams (figure 6). The absorption of LVL is mainly in its transverse direction, parallel to the layers of glue. Assuming a process with only one direction of sorption (height of the beam), and assuming that the relative humidity RH and so the equilibrium moisture content ( $w_{eq}$ ) are expressed by a Fourier series (periodic basis), we can approximate the moisture content  $w$  at a depth  $z$  as follows [6, 21]:

$$w(z) = \overline{w_{eq}} + \sum_{i=2}^5 \exp\left(-\left(\frac{\pi f_i}{\Delta}\right)^{1/2} \left(\frac{h_i}{2} - z\right)\right) \left(\overline{w_{eq_i}} - \overline{w_{eq_{i-1}}}\right) \quad (10)$$

where  $h_i$  is the height of the specimen,  $z$  is the distance from the middle of the beam (figure 6),  $\overline{w_{eq_i}}$  is the equilibrium average moisture content on surface for

the period rank  $i$ ,  $f_i$  is the frequency associated to the period  $i$ ,  $\Delta$  is the diffusion coefficient in the tangential direction (in  $\text{m}^2/\text{s}$ ).  $\Delta$  is the rate at which moisture is transported between opposite faces of a unit cube of a system when there is unit concentration difference between them, it is also called diffusivity

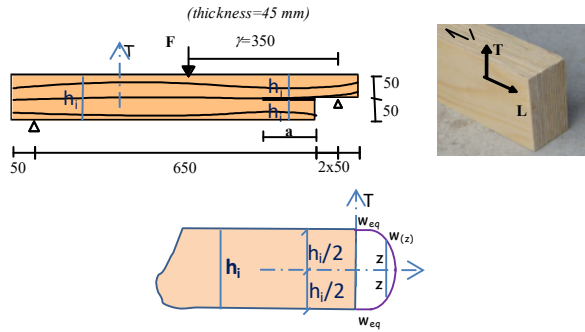


**Figure 6:** Shape of the studied Laminated Veneer Lumber notched beams (dimensions in mm) and an example of evolution of the moisture content  $w(z)$  under the tangential direction ( $a$ : crack length)

Practically, the moisture content  $w(z)$  is determined using four time scales which correspond to periods - hereafter, we have chosen 5 periods enough for wood - along which the averaging value can be processed, namely:  $i = 1$ : year;  $i = 2$ : 3 months (season);  $i = 3$ : month (30.5 days);  $i = 4$ : week (7 days);  $i = 5$ : 1 day. At the first time using equation (10), at time  $t=0$ , the moisture in the specimen is supposed to be uniform and equal to a conditioning moisture  $w_c = w(z) = w_{eq}$ . After, the moisture  $w_{eq}$  varies following LVL isotherm curve and  $w$  varies as expressed by Equation (10).

In this study, RH and thus  $w_{eq}$  are not strictly periodic functions, but their average values are periodic. As an approximation, the relationship (10) can be applied to determine the moisture profile in a notched beam (figure 6). The value of the sorption coefficient  $\Delta$  is taken equal to  $20 \cdot 10^{-11} \text{ m}^2/\text{s}$ , a value we obtained on spruce specimens. In this first approach,  $\Delta$  is supposed not depending on the moisture content or on the temperature and it is also supposed to have the same value during sorption and desorption. The crack surfaces are supposed to be at the equilibrium moisture as external faces; also the moisture evolution above and below the crack is similar to the evolution in beam of height  $h_i$  (figure 6).

### 3 THE VISCOELASTIC CRACK MODELS (VCM)

The purpose is to determine the time-to-failure of timber elements whose rupture is due to the creation and the propagation of a crack (as notched beams, beams with a hole etc...). A damage model is applied to predict initiation (incubation) time; i.e. the time to create a damaged area which leads to the creation of a macro-crack. The propagation of the crack is modeled by a fracture mechanics model considering that the crack

grows in an orthotropic viscoelastic medium and that a damaged area exists at the crack tip [7, 8].

Humidity has adverse effects on these two stages of initiation and crack propagation until failure [9]. These effects must be reproduced by the model. It appears that the lower the moisture is, the shorter the initiation time is. On the other side, the opposite phenomenon is observed for propagation, low moisture leading to a longer propagation time (Figure 8).

#### 3.1 INCUBATION TIME

In the incubation phase, damage appears as a characteristic parameter  $D$  ranging from 0 at the beginning of loading to  $D_c$  at the crack initiation. The deflection of notched beams is calculated by finite element computations with or without a small crack which makes the notch 5 mm longer. Considering that this displacement is proportional to the compliance of the beam, a difference between the displacement with or without a crack can be representative of the damage of the beams. We found, by finite elements calculations,  $D_c=0.01$  for an end notched beam with a crack length equal to 5 mm. Regarding the damage development, the second model of Barrett and Foschi [1], with a non-linear damage evolution and a non-linear cumulative damage, has been chosen:

$$\begin{cases} \frac{dD}{dt} = A \cdot \left( \frac{F(t) - F_0}{F_s} \right)^B + C \cdot D(t) & \text{if } F(t) > F_0 \\ \frac{dD}{dt} = 0 & \text{if } F(t) < F_0 \end{cases} \quad (11)$$

where  $F(t)$  is the applied load,  $F_s$  is the strength of the element at a reference moisture content (hereafter  $w_{ref}=20\%$ ), and  $F_0$  a threshold load.  $A$ ,  $B$  and  $C$  are constants supposed not depending on the moisture, only the threshold load level, noted  $SL_0=F_0/F_s$ , depends on  $w$  (Table 3).

**Table 3:** Parameters used in the incubation model for LVL

w %	9%	20%
A [ $\text{h}^{-1}$ ]	$2,11 \cdot 10^{14}$	$2,11 \cdot 10^{14}$
B	30	30
C [ $\text{h}^{-1}$ ]	0,075	0,075
$SL_0$	0,55	0,60

#### 3.2 PROPAGATION

The crack propagation model is based on the Shapery studies [5] and on the Barenblatt's crack model. In the neighbourhood of the crack, the material is divided into two regions: a process zone which can be highly damaged, nonlinear and viscoelastic and a region surrounding the process zone where the material is considered as linear viscoelastic orthotropic. The crack length speed ( $da/dt$ ) is given by the Equation (12). Details on the determination of the formula are developed in [7].

$$\frac{da}{dt} = \frac{\pi}{2} \left[ \frac{C_2 \lambda_n}{(K_{Ic}^2 - K_I(a)^2)} \right]^{1/n} \frac{K_I(a)^{2(1+1/n)}}{(\sigma_m I_1)^2} \quad (12)$$

where:

-  $K_I(a)$  is the stress intensity factor in opening mode I, depending on the crack length  $a$  (figure 7)

$$K_I = \frac{F}{b\sqrt{\gamma}} g\left(\frac{a}{\gamma}\right) \quad (13)$$

- $K_{Ic}$  is the critical stress intensity factor,
- $I_1$  represents the distribution of the cohesive stress at the crack tip,
- $\sigma_m$  is the maximum of the cohesive stress
- the parameter  $\lambda^n$  is a function of the viscosity of the material,
- the parameters  $C_0$ ,  $C_2$  and  $n$  are coefficients depending on the material viscoelastic properties.

**Table 4:** Parameters used in the propagation model for LVL

w %	9%	20%
$C_0$ [MPa <sup>-1</sup> ]	2.03E-3	2.98E-3
$C_2$ [s <sup>-n</sup> ]	1.22E-2	1.55E-2
$n$	0,41	0,38
$\lambda_n$	0,64	0,66
$\sigma_m I_1$ [MPa]	50	45
$K_{Ic}$ [MPa√m]	0,66	0,54

Figure 7 presents the evolution of the calibration function for these LVL notched beams for both moistures  $w$ .

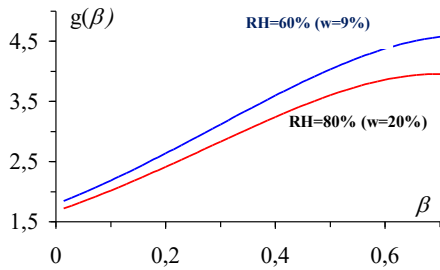


**Figure 7:** Analysis model Calibration function  $g$  versus the reduced crack length  $\beta=a/\gamma$  ( $\gamma=350$  mm)

When moisture varies, all parameters are supposed to vary linearly with the average moisture content (variation deduced from the values of Table 4), excepted for  $\sigma_m$  and  $I_1$ . As the crack tip is supposed to be at the equilibrium moisture  $w_{eq}$ , it was considered that  $\sigma_m I_1$  varies with the equilibrium moisture  $w_{eq}$ . This moisture is obtained using recorded RH and wood sorption curve at the temperature 20°C. When the moisture content is greater than saturation moisture (here fixed at  $w_s = 25\%$ ), the parameters take the values corresponding to the moisture at saturation  $w_s$ .

## 4 TIME MODELLING

Simulations are realised for more than thousand scenarios of Atlantic, Auvergne, Brittany and Corsica climates at two conditioning RH:  $RH_c = 55\%$  ( $w_c = 9\%$ ) and  $RH_c = 80\%$  ( $w_c = 20\%$ ) (Figures 8 and 9). At the end of the conditioning, the beams are supposed to be in a homogeneous state of moisture  $w_c$ . In this paper, since the strength is linked to the moisture, the stress level is defined as the ratio between the applied load and the strength at a reference moisture content (here  $w_{ref} = 20\%$ ) and it is noted  $SL_r$ .

Predictions of the proposed model for various air humidity simulations are compared with creep test results carrying on notched LVL beams under various climatic conditions near Bordeaux. Correct trend of the experimental results is obtained as illustrated in Figure 8.

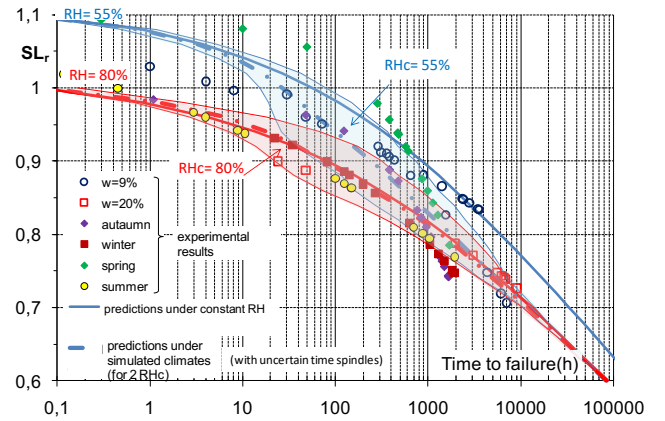


**Figure 8:** Experimental time to failure and average predictions of VCM under 10 000 RH simulations of Atlantic climates. ( $RH_c$ : conditioning RH-  $SL_r$ : creep stress level)

As observed on Figures 8 and 9, for a given stress level, the time to failure is a little higher when the moisture is smaller. A beam conditioned in a wet area has also a delayed crack than if it is conditioning at  $RH_c = 55\%$ , the influence of conditioning however decreases for low stress levels.

Figure 9 emphasizes the influence of the considered regions on the duration of load. Considering the two extreme French regions (Brittany and Corsica), for high stress level  $SL_r$ , (up than 0.6), the incubation time is more influenced by the conditioning moisture than by the climate; only propagation time is depending on the region. For example at  $SL_r = 0.8$ , for an initial moisture  $w = 9\%$  ( $RH_c = 55\%$ ), the estimated time to failure in Brittany is around 70 days and in Corsica is 200 days; for both the incubation is one day. For an initial moisture equal to 20% ( $RH_c = 80\%$ ), the average lifetime is 40 days in Brittany, 122 days in Corsica, with both 3 days incubation. In terms of lifetime, it is seems however preferable to have a beam exposed to a dry environment.

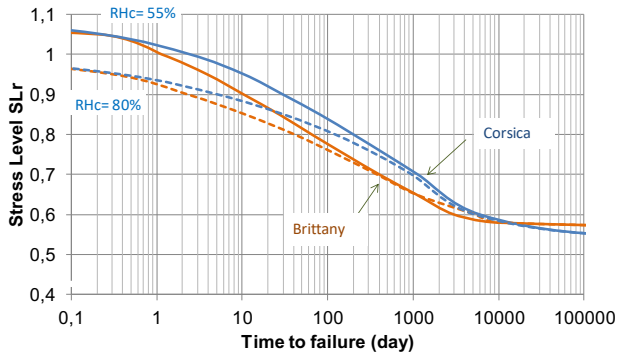


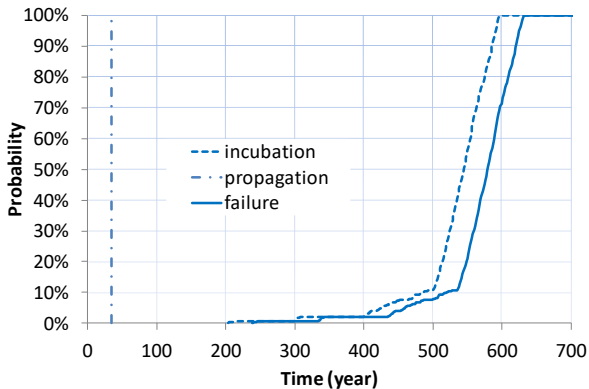
**Figure 9:** average predictions of VCM under 10 000 RH simulations of Brittany and Corsica climates. (RHc: conditioning RH- SLr : creep stress level). Full line: RHc=55%, dotted line RHc=80%

When the stress level is smaller than 0.6, because of the considered threshold load level (Table 3), when the relative humidity is elevated, like in Brittany, the crack initiation becomes longer, and when the stress level is smaller or equal to 0,55, this time is almost infinite (longer than 600 years). This phenomenon is ever more emphasizes than the initial moisture is high (Table 5).

**Table 5:** Average and standard deviation (St dev) predictions for Mediterranean French climate (Creep load at a stress level = 0.55), for two conditioning RHc

Time (year)	RHc=55%		RHc=80%	
	Average	St dev	Average	St dev
Incubation	535	55	547	28
propagation	35	0	35	0
failure	569	55	582	28

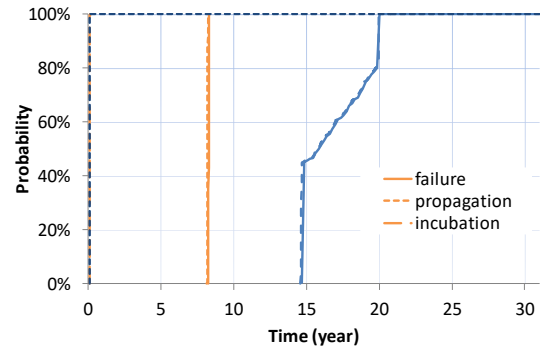
Figure 10 presents the probability of failure at a stress level equal to 0.55 in Corsica (initial moisture  $w_c=9\%$ ): this lifetime is strongly dependent on the incubation time.



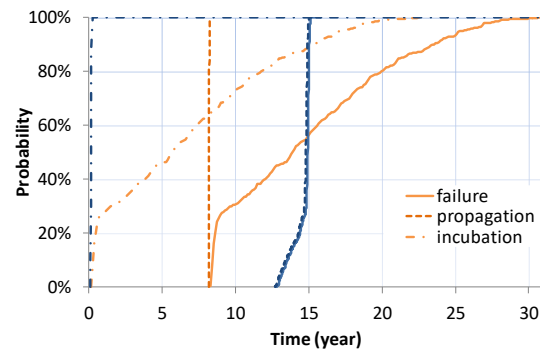
**Figure 10:** Time probability of notched beam under Corsica climate (RHc: conditioning RH = 55%) - Creep at a stress level = 0.55.

Figure 11 presents the time probability of incubation, propagation and failure of notched beams under Brittany and Mediterranean climates for two extreme initial

moistures  $w_c=9\%$  ( $RH_c=55\%$ ) and  $w_c=20\%$  ( $RH_c=80\%$ ), for a creep stress level equal to 0.6.



(a)



(b)

**Figure 11:** Time probability of notched beams under two extreme French regions: clear line: Brest, dark line: Ajaccio (RHc: conditioning RH (a) = 55% - (b) = 80%) – (Creep at a stress level = 0.6)

Table 6 also presents the influence of the initial moisture in two French regions. In Brittany, if notched beams are conditioning under high relative humidity, the incubation time become as long than the propagation time and the time to failure increases. In Corsica, only the propagation time is affected by the conditioning moisture, it is lower when the initial moisture is high.

**Table 6:** Average and standard deviation (St dev) predictions for two extreme French climates at two conditioning RHc (Creep at a stress level = 0.6)

RHc=55%	Brittany		Corsica	
Time (year)	Average	St dev	Average	St dev
Incubation	0,08	0,004	0,08	0,000
propagation	8,19	0,014	16,66	2,208
failure	8,27	0,014	16,74	2,208

RHc=80%	Brittany		Corsica	
Time (year)	Average	St dev	Average	St dev
Incubation	6,53	5,716	0,12	0,005
propagation	8,20	0,013	14,53	0,590
failure	14,73	5,718	14,65	0,589

Based on the simulations, beams with an initial crack exposed in a dry land have delayed cracking compared to a wet climate. Simulations time to failure obtained using real recorded relative humidity are similar to thus obtained with the simulated climates.



## 5 CONCLUSION

Combined models for temperature and humidity fluctuations have been built after an in-depth analysis of real data sets for four French climates. The models are able to reproduce: the seasonal variations for both variables, the day/night fluctuations, with cycles in the T-HR diagram, reproducing the humid air physics, and the time correlation of signals. A time scale of 5-7 days has been identified.

The lifetime model developed predicts the incubation time and the time of crack propagation until failure. A damage model is applied to predict initiation (incubation) time; i.e. the time to create a damaged area which leads to the creation of a macro-crack. The propagation of the crack is modelled by a fracture mechanics model considering that the crack grows in an orthotropic viscoelastic medium and that a damaged area exists at the crack tip. In the case of cracking failure of a notched beam, we have distinguished the two stages of initiation and of crack propagation until failure, since humidity has adverse effects on these two stages. The crack initiation time increases when the humidity is high. On the other side, the opposite phenomenon is observed for propagation, low moisture leading to a longer propagation time. For a given stress level, the time to failure is a little higher when the moisture is smaller. Based on the simulations, beams with a initial crack exposed in a wetland have early cracking compared to a dry climate.

Based on simulation and some experiments, in terms of lifetime, it is preferable to have a beam exposed to a dry environment excepted if the beam, without initial crack, is submitted to a smaller stress level (smaller than 0.6), in this case, a wet area leads to a longer time to failure because the incubation time is very longer.

The same model will be used now to compare the response of components located in different environments, corresponding to common environments in metropolitan France. A further use of this modeling will be to simulate various realistic climate change scenarios and to quantify their effects on component lifetime, structure reliability, such as to predict possible increase in maintenance costs due to global change scenarios.

## REFERENCES

- [1] Barrett J.D., Foschi R.O.: Duration of load and probability of failure in wood. Part I. Modelling creep rupture. *Can. J. Eng.*, vol. 5, 505-514, 1978.
- [2] Bilbao J., De Miguel A.H., Kambezidis H.: Air temperature model evaluation in the North Mediterranean belt area, *J. Applied Meteorology*, 41, 872-881, aug. 2002.
- [3] Breyse D., Chaplain M., Marache A., Malaurent P.: Random temperature and humidity models in Atlantic environment. *European Journal of Civil and Env. Engineering*, 15:1045-1058, 2011.
- [4] Brockway G.S, Schapery R.A.: Some viscoelastic crack growth relations for orthotropic and prestrained media. *Engineering Fracture Mechanics*, 10:453-468, 1978.
- [5] Castera P. : Modélisation du comportement d'une pièce de bois soumise à des gradients évolutifs d'humidité. Thèse de doctorat, Université Bordeaux 1, 1987.
- [6] Chaplain M., Valentin G.: Fracture mechanics models applied to LVL beams delayed failure. *Holz als Roh- und Werkstoff*, vol. 65 (1), 7-16, 2007.
- [7] Chaplain M., Valentin G., Chateaufneuf A.: Modelling relative humidity effect on load duration of timber beams. *Proceedings of WCTE 2008 - 10th World Conference on Timber Engineering*, Miyazaki, Japan, 2-5 june 2008.
- [8] Chaplain M., Breyse D., Marache A., Modelling time to failure of notched beams under random humidity variations of Atlantic environment, *Eur. Journal of Civil and Env. Engineering*, 15:1059-1072, 2011.
- [9] Gustafsson P.J., Hoffmeyer P., Valentin.G., DOL behaviour of end-notched beams, *Holz als Roh - und Werkstoff*, 56, 307-317, 1998.
- [10] Häglund M., Isaksson T., Holst J.: Time-series modeling of moisture exposure on timber structures. *Building and Environment*, 42:1515-11521, 2007.
- [11] Hartley I.: Wood: Moisture Content, Hygroscopicity, and Sorption. *Encyclopedia of Materials: Science and Technology*, Elsevier Science Ltd, 9668-9673, 2001.
- [12] Isaksson T., Thelandersson S., Ekstrand-Tobin A.: Johansson P., Critical conditions for onset of mould growth under varying climate conditions. *Build. and Envir.*, 43:1712-1721, 2010.
- [13] JCSS, Probabilistic model code, Part 2: loads, <http://www.jcss.ethz.ch>, accessed on 2010, oct. 4<sup>th</sup>.
- [14] Johnson G.L., Hanson C.L., Hardegree S.P., Ballard E.B.: Stochastic weather simulation: overview and analysis of two commonly used models. *J. Appl. Meteor.*, 35:1878-1896, 1996.
- [15] Jönsson J.: Internal stresses in the cross-grain direction in glulam induced by climate variations. *Holzforschung*, 58:154-159, 2004.
- [16] Parton W.J., Logan J.A.: A model for diurnal variation in soil and air temperature. *Agricultural meteorology*, 23:205-216, 1981.
- [17] Ranta-Maunus A.: Effects of climate and climate variations on strength, S. *Thelandersson and H.J. Larsen ed., Timber engineering*, Wiley, New York, Chapter 9, 153-167, 2003.
- [18] Reicosky D.C., Winkelman L.J., Baker J.M., Baker D.G.: Accuracy of hourly air temperatures calculated from daily minima and maxima. *Agric. For. Meteor.*, 46:193-209, 1989.
- [19] Semenov M.A., Brooks R.J., Barrow E.M., Richardson C.W.: Comparison of the WGEN and LARS-WG stochastic weather generators for diverse climates. *Climate Res.*, 10 : 95-107, 1998.
- [20] Valentin G., Chaplain M., Chateaufneuf A., Castéra P., Galimard Ph.: ACI Risque et Génie Civil Bois: Le bois dans la construction en France peut-il faire face aux nouveaux risques climatiques?, 128p, 2007.